Molecular Monolayers Enhance the Formation of Electrocatalytic Platinum Nanoparticles on Vertically Aligned Carbon Nanofiber Scaffolds

ARTICLE *in* THE JOURNAL OF PHYSICAL CHEMISTRY C · MAY 2007

Impact Factor: 4.77 · DOI: 10.1021/jp070102c

3 AUTHORS:

Kevin M Metz
Albion College
16 PUBLICATIONS **382** CITATIONS
SEE PROFILE

Divya Goel
VIT University
11 PUBLICATIONS **106** CITATIONS
SEE PROFILE

Robert J. Hamers
University of Wisconsin–Madison
382 PUBLICATIONS **17,101** CITATIONS
SEE PROFILE

Molecular Monolayers Enhance the Formation of Electrocatalytic Platinum Nanoparticles on Vertically Aligned Carbon Nanofiber Scaffolds

Kevin M. Metz, Divya Goel, and Robert J. Hamers*

Department of Chemistry, University of Wisconsin−Madison, 1101 University Avenue, Madison, Wisconsin 53706

Received: January 5, 2007; In Final Form: February 14, 2007

We demonstrate the use of molecular monolayers to enhance the nucleation of electrocatalytically active platinum nanocrystals onto vertically aligned carbon nanofiber (VACNF) scaffolds. The photochemical functionalization of VACNFs with bifunctional organic alkenes produces monolayer-modified VACNFs exposing large amounts of carboxylic acid groups. Subsequent electroless deposition of platinum leads to high densities of ∼8 nm diameter Pt nanocrystals uniformly deposited along the length of the nanofibers. Electrochemical measurements show that the molecular monolayers do not impede redox behavior of the electrode, and measurements of the electrocatalytic oxidation of methanol show very high catalytic efficiency. Our results suggest that the use of molecular functionalization layers provides an improved way to integrate nanostructured carbon with metals for a variety of catalytic and electrocatalytic applications.

Introduction

One of the key challenges in nanoscience is the integration of different nanoscale materials having distinct chemical or physical properties to form novel types of hybrid materials with unique functionality. Nanostructured forms of carbon are of great interest because of their excellent thermal stability and electrical conductivity combined with their ability to form very high surface area electrodes.[1−4] While carbon is quite inert, the deposition of nanocrystalline metals onto carbon nanofibers and carbon nanotubes presents unique opportunities to fabricate new types of hybrid electrode structures that combine the high stability and electrical conductivity of carbon with the catalytic properties of transition metals; such hybrid materials are of great interest for applications such as electrocatalytic electrodes in fuel cells.[1,5−9]

Vertically aligned carbon nanofibers (VACNFs)[10] are an especially promising form of nanoscale carbon. The vertical orientation provides high accessibility to the interstices between fibers, and each nanofiber has a direct electrical contact to an underlying metal electrode, thereby minimizing contact resistances. Furthermore, the growth of VACNFs via plasma-enhanced chemical vapor deposition commonly leads to nanofibers having a stacked-cup structure that exposes large amounts of edge-plane graphite along the nanofiber sidewalls.[11−14] Since electron-transfer rates at edge-plane sites are orders of magnitude faster than at basal plane sites,[14,15] this suggest that VACNFs may be excellent substrates for integration with catalytic nanocrystalline metals. While metals can be deposited directly onto VACNFs,[9] the density of particles and their adhesion depend strongly on the number of oxidized surface sites, which is often low. The density of metallic nanocrystals can be improved by oxidation to provide carboxylic acid and other chelating surface groups.[5,9,16] However, the conditions needed for this oxidation typically involve exposure to strong acids (e.g., boiling nitric acid) that leave behind a broad distribution of oxidized types,[17] only some of which are effective in chelating to metals. Furthermore, the harsh conditions are not readily compatible with the underlying metal electrode structures needed for electrical contact to the nanofibers.

Recent studies have demonstrated that the various forms of carbon, including VACNFs, can be functionalized with molecular layers bearing an alkene group via illumination with 254 nm light.[18−20] Using molecules with a second functional group, such as a carboxylic acid or methyl ester (a precursor to carboxylic acids), provides a means to selectively tune the chemical and physical properties of carbon via covalent molecular functionalization. Recently, it was shown that functionalization of VACNFs with molecules bearing carboxylic acid groups greatly enhances the deposition of gold onto VACNF scaffolds.[21] This work suggests that similar approaches might be useful for forming electrocatalytic structures that link the catalytic reactivity of transition metals such as Pt with the unique properties of nanoscale carbon. Yet, the ability of molecular layers to enhance nucleation of catalytic nanoparticles while also providing the electrical conductivity needed for effective electrocatalysis has not been demonstrated previously.

Here, we report a new approach for fabricating nanoscale hybrid electrodes using molecular functionalization layers to enhance the nucleation of platinum nanoparticles onto VACNF electrodes via electroless deposition. Our results demonstrate that molecular functionalization layers can provide a homogeneous, high density of binding sites that enhance nucleation of nanocrystalline metals onto VACNF electrodes without adverse impact on the electron-transfer processes. The resulting Pt/nanofiber nanocomposites retain high electrocatalytic activity, as demonstrated through their ability to achieve facile electrocatalytic oxidation of methanol.

Experimental Methods

Vertically aligned carbon nanofibers were grown in a custom-built chamber using DC plasma-enhanced chemical vapor deposition (DC-PECVD)[10,12,13,22] with acetylene and ammonia

* To whom correspondence should be addressed. E-mail: rjhamers@wisc.edu.

10.1021/jp070102c CCC: $37.00
Published on Web 04/27/2007

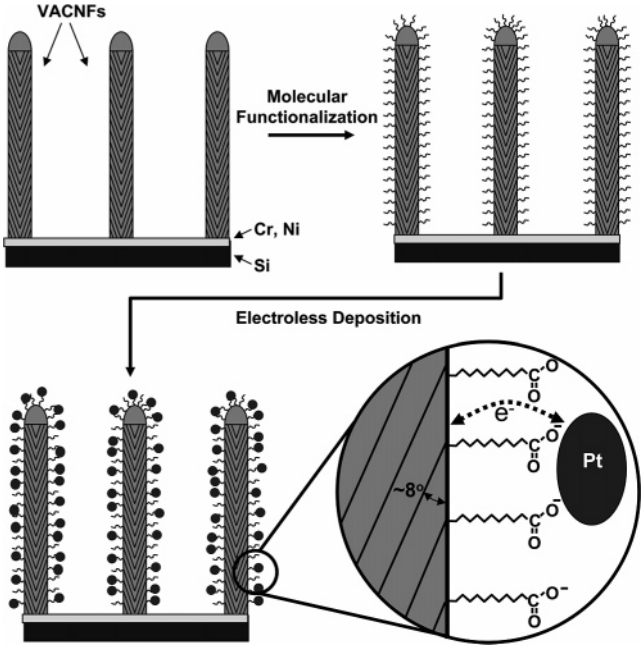

Figure 1. Schematic illustration of the process used to nucleate platinum nanoparticles on vertically aligned carbon nanofibers (VACNFs).

as reactants. Fibers were grown on highly doped silicon substrates coated with a metal bilayer consisting of 20 nm of chromium followed by 20 nm nickel, which acts as a catalyst. Growth conditions used here[22] produced high densities of cylindrical, vertically aligned fibers with diameters of ~70−100 nm and an average length of 2 μm. Transmission electron microscopy (TEM) images collected from fibers grown in our lab[23] show that the fibers are in the stacked-cup geometry.[11,13] TEM images show that the graphene sheets make an angle with respect to the fiber axis of ~8°, leaving an edge-plane site exposed every 2−3 nm along the fiber sidewalls.

Results

Figure 1 depicts the procedure used here to deposit platinum nanocrystals on the sidewalls of the carbon fibers. In contrast to most previous studies of metal−nanofiber hybrids, we use electroless deposition, which involves the catalytic deposition of a metal from a metastable solution. Electroless deposition was chosen because the rate of nucleation can be easily controlled to provide uniform deposition along the length of the nanofibers. The specific procedure used here for Pt deposition is based on methods developed for deposition on plastics[24] that we have adapted for nanocrystals on nanofibers. A critical aspect of electroless deposition is the chelation of metals to carboxylic acid groups on the surface of interest to initiate the catalytic deposition from solution. To achieve high densities of carboxylic acid groups, we use a procedure recently developed in our laboratory in which organic molecules bearing a terminal alkene (C═C) group are photochemically linked to the surfaces of carbon nanofibers[19] upon illumination with ultraviolet light at 254 nm. By linking a methyl ester to the surface and then exposing to basic conditions, very high densities of carboxylic acid groups are formed.

Functionalization was accomplished by dripping on a small amount of undecylenic acid methyl ester onto the sample and illuminating with 254 nm light (~0.4 mW/cm^2) for 16−18 h. This functionalization step was monitored using infrared reflection−absorption spectroscopy (IRRAS) on a Bruker Vertex 70 FTIR spectrometer. Figure 2 shows an IRRAS spectrum (500 scans at 4 cm^{-1} resolution, 60° incidence angle, with s-polarized light) of the CH-stretching and C═O stretching regions; in these measurements, a sample of bare nanofibers was used as a reference. After functionalization, the spectrum shows a strong peak at 1730 cm^{-1} arising from the stretching mode of the carbonyl group of the methyl ester. There are also new peaks at 2856 and 2929 cm^{-1} corresponding to the CH_2 asymmetric and symmetric stretching modes and a shoulder (2962 cm^{-1}) corresponding to the CH_3 vibration of the terminal methyl group. Additional measurements (not shown) of infrared peaks confirm that the functionalization is nearly complete within ~8 h. To ensure the maximum coverage, we typically use a longer time of ~16 h. After linking the methyl ester to the surface, it was converted to a terminal carboxylic acid group in a 250 mM slurry of potassium tert-butoxide in dimethyl sulfoxide (5 min),[19] producing a surface with a high density of carboxylic acid groups.

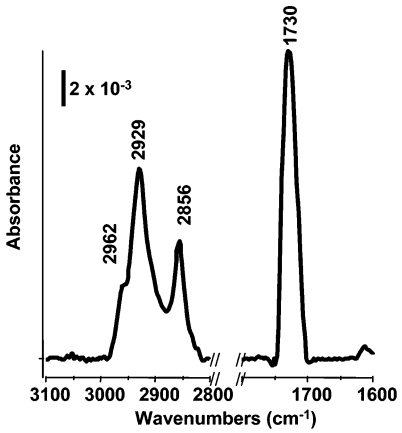

Figure 2. Partial IRRAS spectrum of undecylenic acid-methyl ester modified carbon nanofibers.

Formation of Pt nanocrystals on the acid-terminated sample was achieved using a three-step electroless deposition procedure.[24] The carboxylic acid modified fibers were first sensitized with tin.[25] The tin-sensitized fibers were then immersed in a 0.03 M solution of palladium chloride, which leaves palladium atoms bound to the surface following a redox reaction with the tin ions. Finally, the fibers were immersed in a Pt electroless deposition[26] at 55 °C and were left for 1−3 h. The platinum loading was determined by dissolving the platinum nanoparticles off the fibers into a known volume of aqua regia and measuring the solution concentration with inductively coupled plasma optical emission spectroscopy (ICP-OES). Using this procedure, platinum loadings between 1 and 7 μg/cm^2 were obtained, depending on the time in the deposition bath.

Many previous studies of organic monolayers on gold,[27,28] silicon,[29−31] and diamond[32] have shown that dense monolayers can act as barriers to electron transport. However, the VACNF sidewalls are chemically heterogeneous because of the presence of both highly reactive edge plane and less reactive basal plane exposed along the sidewalls, suggesting that even though the monolayers are self-terminating, they are likely disordered and inhomogeneous. To evaluate whether the monolayer impedes electron transfer, cyclic voltammetry measurements were performed. Figure 3 shows cyclic voltammograms (CVs) using samples of bare (nonfunctionalized) carbon fibers and carbon fibers that were functionalized with a carboxylic acid monolayer as described above. The voltammograms were collected using a scan rate of 25 mV/s in a three-electrode geometry, with a Ag/AgCl reference electrode (3 M KCl filling solution), in a

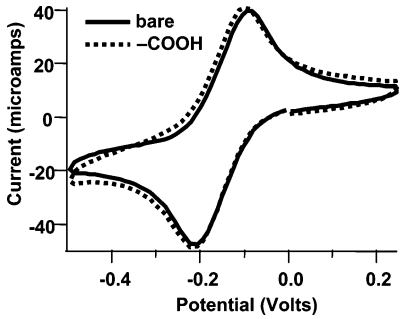

Figure 3. Cyclic voltammograms of bare (solid) and carboxylic acid modified (dotted) carbon nanofibers in 4 mM $Ru(NH_3)_6^{2+/3+}$ in 0.1 M KCl, collected at 25 mV/s scan rate. All potentials are referenced to the standard hydrogen electrode.

solution of 4 mM $Ru(NH_3)_6^{2+/3+}$ in 100 mM KCl. The ruthenium hexamine redox couple was selected because it has been shown to be an outer sphere redox couple that is sensitive to the electronic structure (density of states) of the electrode and not sensitive to surface impurities and functional groups.[33,34] Figure 3 shows that the organic functionalization layer has very little impact on the electron-transfer reactions. In particular, the diffusion-limited current at high potentials is nearly identical before and after functionalization, and the separation between oxidation and reduction peaks is 112 mV for the bare carbon nanofibers and 107 mV for the functionalized carbon nanofibers. This peak separation is approximately twice the expected value for a fully reversible fast redox process but is smaller than the value of ~120 mV reported on hydrogen-terminated glassy carbon.[35,36] Notably, the peak separations are nearly identical between the bare and functionalized carbon nanofiber electrodes, indicating that the presence of the monolayer does not affect the electron-transfer kinetics. This is consistent with recent studies that have shown monolayers formed as described here allow facile redox reactions of species in solution.[20]

Figure 4a shows a scanning electron microscope image of typical carbon nanofibers decorated with platinum nanoparticles produced using this method. It is clear from Figure 4a that the platinum nanoparticles are uniformly distributed along the length of the fiber and have a high density. In a few cases, a gradient was observed along the length of the fiber with a higher density of nanoparticles near the tip of the fiber than near the base; however, the vast majority of samples show very uniform distributions of nanoparticles along the length. The observed gradients were generally located in region of high nanofiber densities and most likely arise from shadowing during the ultraviolet functionalization step. Figure 4b shows a transmission electron microscope image of platinum nanoparticles on a single carbon nanofiber. This image illustrates the high densities of platinum nanoparticles that can be deposited using this method. Figure 4c shows another transmission electron microscope image of platinum nanoparticles on a single carbon nanofiber. Analysis of the TEM images shows that the platinum nanoparticles deposited are 8 ± 1 nm in diameter. This is significant because nanoparticles between 3 and 10 nm are optimal for the electrocatalytic oxidation of methanol by carbon-supported Pt catalysts.[37] While many of our deposited particles appear to have well-defined shapes that are consistent with crystalline growth, electron-diffraction patterns collected from a small number of single platinum nanoparticles (not shown) showed a ring pattern, suggesting that the deposited particles may be polycrystalline.

To identify what effect the organic monolayer has on the density of Pt nanoparticles, control experiments were performed using bare (nonfunctionalized) carbon nanofibers. In these

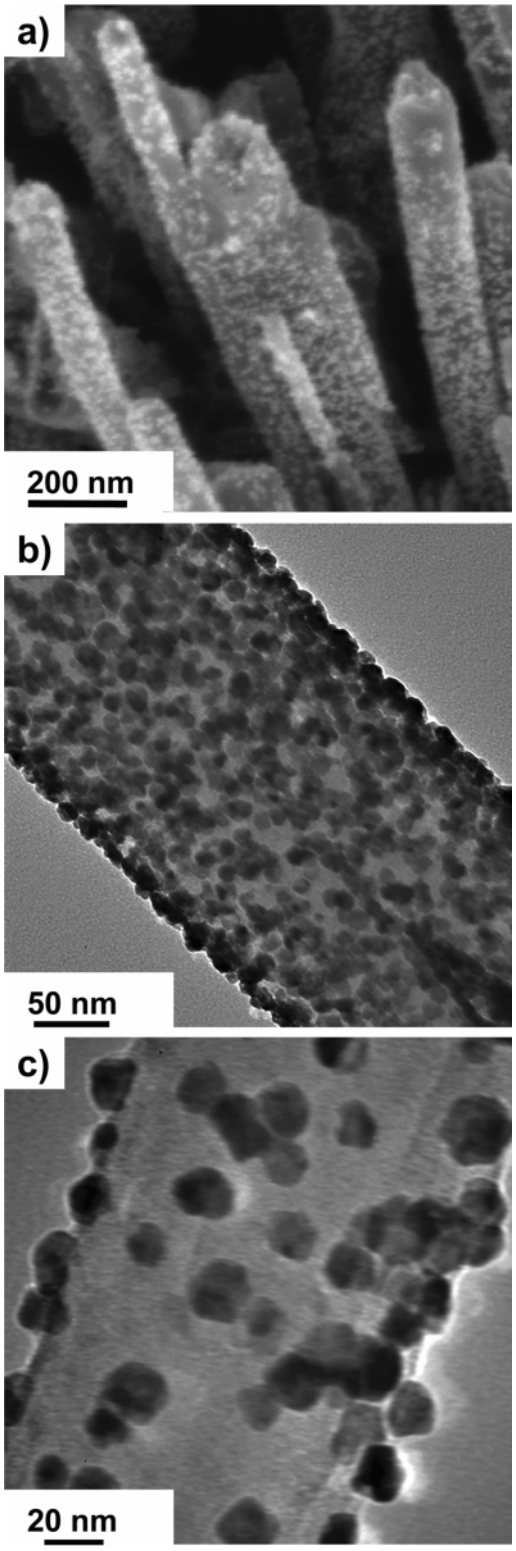

Figure 4. (a) SEM image of platinum nanoparticles on carbon nanofibers. (b, c) TEM images of platinum nanoparticles on a single carbon nanofiber.

experiments, bare fibers were wet in methanol and otherwise were handled identically to the functionalized fibers for the metal deposition procedure. Scanning electron microscopy (SEM) analysis showed low densities of nonuniformly distributed platinum nanoparticles with smaller diameters than the platinum particles deposited on functionalized carbon nanofibers. ICP-OES analysis revealed a Pt loading of 0.4 $\mu g/cm^2$ for the control samples, approximately 10−20 times less than what was

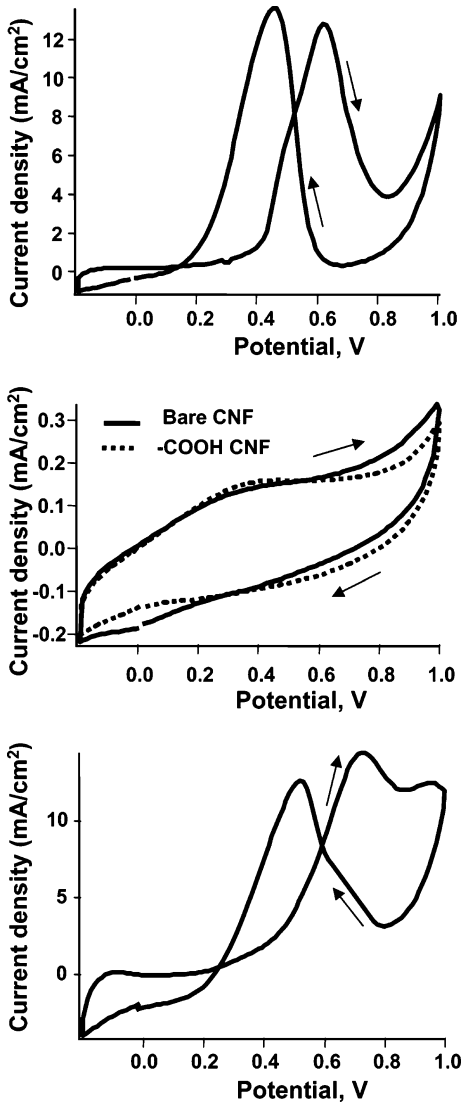

Figure 5. Cyclic voltammograms of (a) platinum modified carbon nanofibers, (b) bare (solid) and carboxylic acid modified (dotted) carbon nanofibers, and (c) 60 wt % platinum on XC-72 activated carbon. All measurements were performed in 0.5 M H_2SO_4 and 1 M methanol, collected at 25 mV/s scan rate, referenced to the standard hydrogen electrode.

obtained on the functionalized samples. Since electroless deposition requires carboxylic acid groups to chelate the metals, we presume that a small amount of residual deposition on nonfunctionalized samples likely arises from a small number of oxidized surface sites or possibly as a result of inherent instabilities common in electroless platinum baths.[24] A comparison of the density of Pt nanoparticles on the bare and functionalized nanofibers showed that the functionalization leads to a very pronounced enhancement in the nucleation of Pt onto the nanofibers.

A key factor to the practical application of platinum−carbon composites is electrocatalytic activity. To examine the electrocatalytic activity of the nanocrystalline Pt/nanofiber composites, we utilized the oxidation of methanol, $CH_3OH + H_2O \rightarrow CO_2 + 6H^+ + 2e^-$. This reaction is of great interest for use in direct methanol fuel cells.[9,16,38] Figure 5a shows results obtained for the methanol oxidation reaction using platinum-modified VACNFs as the working electrode. The electrode was conditioned by cycling between −0.2 to 1 V at a scan speed of 100 mV/s until a steady state was achieved (at least 25 cycles) in a solution consisting of 0.5 M sulfuric acid and 1 M methanol. The methanol oxidation reaction was then observed by cycling over the same potential range at a scan rate of 25 mV/s. The resulting cyclic voltammogram in Figure 5a is similar to those reported in the literature.[16,39,40] On the forward sweep, a peak is observed near 0.6 V that arises from the partial oxidation of methanol, $CH_3OH \rightarrow CO + 4H^+ + 4e^-$.[41,42] This reaction produces CO that, in turn, can poison the reaction.[43] Several intermediates can also be formed in this initial oxidation, but these comprise a small percentage of the products and are converted to CO_2 once the system reaches a steady state.[41] On the reverse sweep, a second oxidation peak is observed near 0.4 V. This peak arises from the oxidation of CO to produce CO_2, $CO + H_2O \rightarrow CO_2 + 2H^+ + 2e^-$.[42] This step restores the free surface for methanol adsorption. Additional kinetic pathways are also possible, but these are minor reactions under the conditions used here.[41,42] These data demonstrate that the Pt nanocrystals formed on the functionalized nanofibers have good electrocatalytic properties. Importantly, the presence of an intermediate molecular layer does not inhibit their electrocatalytic activity.

For comparison, Figure 5b shows results of control experiments performed on bare (as-grown) nanofibers and on nanofibers after functionalization to expose carboxylic acid groups. The curves show no significant redox activity and are dominated by the capacitance of the electrodes. This confirms that the catalytic activity in Figure 5a is associated with the platinum and not with graphite edge planes or other reactive sites associated with the nanofibers or the functionalization layers.

Finally, in Figure 5c, we show similar voltammetry experiments performed on a conventional Pt/C conventional electrode that was made using a commercially available Pt/C catalyst Vulcan XC-72 with a 60 wt % platinum loading (Fuel Cell Store). The electrodes were created by dispersing 5 mg of the platinum/Vulcan catalyst in 1 mL of isopropyl alcohol via ultrasonication for 30 min to create a carbon "ink".[16] This carbon ink was then placed onto a nickel, chromium-coated silicon substrate, identical to those used here for carbon nanofiber growth, and the alcohol was evaporated at room temperature. Ten microliters of a 5 wt % Nafion solution was then added to the top of the deposited platinum on carbon to help keep the carbon in contact with the metal underlayer during testing. The electrodes were conditioned and were tested identically to the platinum-on-carbon nanofibers as described above.

A comparison of the voltammograms for Pt-on-nanofibers samples (Figure 5a) and the Vulcan Pt/C (Figure 5c) shows important similarities and differences. First is that both samples yield similar peak currents, despite having very different platinum loadings. For example, the bulk Pt/C material with an average platinum loading of 250 μg/cm^2 yielded a peak current density of 14.4 mA/cm^2, at 0.72 V, while the platinum-on-nanofiber samples with an average loading of only 7 μg/cm^2 yielded a peak current density of 12.8 mA/cm^2 (at 0.61 V). Thus, the Pt/nanofiber composites are approximately 30 times more efficient in their use of Pt compared with the bulk Pt/C electrodes. Second, there is a shift in the potential at which the peak current arises: 0.72 V for the Pt/C bulk material and 0.61 V for Pt/nanofiber samples. This shift could result from differences in the distribution of exposed Pt crystal faces exposed on the two samples[44] or from increased contact resistance in the Pt−Vulcan sample created by the use of a powder on a planar metal electrode held in place with a Nafion layer.

With increased scan speeds, it was noticed that the Nafion layer would delaminate. Similar delamination due to rapid evolution of the reaction product CO_2 has been reported

previously and is a major factor limiting the lifetime of direct methanol fuel cells.[45] In contrast, the Pt-on-nanofiber samples were stable under identical conditions. Our data demonstrate that the Pt-on-nanofiber samples prepared as described here provide improved stability and the ability to oxidize methanol at lower applied potentials (0.61 V vs 0.72 V) than commercial Pt−Vulcan.

Discussion

The above results demonstrate several important points. First, they demonstrate that the use of a molecular functionalization layer can greatly enhance the nucleation of nanocrystalline metals onto carbon nanofibers by providing large numbers of carboxylic acid groups on the surface. Second, they show that the molecular layers do not necessarily act as blocking layers for electron transport, with the result that electron-transfer reactions to redox species in solution and the adsorbed nanoparticles are facile. Finally, they demonstrate that nanocrystalline metals deposited onto the molecular layers exhibit excellent electrocatalytic activity, as evidenced by their ability to facilitate the methanol oxidation reaction. While for practical applications such as fuel cells more complex catalytic materials (often Pt/Ru mixed catalysts) are typically used, these results suggest that the use of molecular functionalization layers may provide a versatile means for fabricating and controlling nanostructured electrocatalytic electrodes.

The use of molecular functionalization layers is significant because the electroless deposition requires chelation of metals to the electrodes. While many previous studies have noted that efficient metal deposition is strongly dependent on the presence of high concentrations of oxidized surface sites,[5,9,16] the harsh chemical oxidation procedures typically create an inhomogeneous distribution of different types of oxidized carbon,[17] only some of which are effective at chelating metals. The photochemical functionalization procedure used here provides a very high density of carboxylic acid sites and also avoids the corrosion and delamination issues associated with the harsh oxidizing conditions used previously.

Of greater intrigue is the fact that the molecular layer does not impede electron transfer between the carbon nanofibers and the Pt nanoparticles or to $Ru(NH_3)_6^{2+/3+}$ species in solution. This is unexpected, because most previous studies of surface monolayers have reported that dense monolayers typically block or inhibit electron transfer.[28,29,31] On carbon surfaces, the formation of strong covalent bonds between the nanofibers and the molecular layers likely prevents lateral diffusion of molecules and provides a way to controllably tune the coverage. While our experiments indicate that the molecular layer formation is complete after <8 h, it is likely that the organization of the layers is complex because of the heterogeneity of the nanofiber surfaces. Transmission electron microscope images of our fibers show a stacked-cup arrangement that exposes an edge plane every $\sim 2-3$ nm along the length of the nanofibers as depicted in Figure 1. The exposure of these edge-plane sites is important in two respects. First, since edge sites are known to be more reactive than basal plane sites,[14,15,46] the photochemical functionalization reaction may preferentially bind molecules at the edge-plane sites. This would leave the basal plane regions bare or functionalized at a lower density, thereby providing porosity toward electroactive species or the deposited metals. Second, the much faster rate of electron transfer at edge-plane compared with basal-plane sites[14,15] directly facilitates electron transfer.

At the present time, it is not possible to determine whether the molecular layer completely separates the nanoparticles from the nanofiber (as depicted in Figure 1) or whether Pt atoms within the particles may form a direct bridge to the nanofiber, providing a more direct electrical connection between the nanofiber and the Pt nanocrystals. Further research will be needed to fully understand the mechanism of electron transfer in these complex nanostructured materials. However, it is clear that the use of molecular layers provides a way to tune the properties of VACNF electrodes to enhance the nucleation of electrocatalytic nanocrystals without adverse impact on the electron-transfer properties of the nanocrystal−nanofiber interface, thereby facilitating the fabrication of novel types of catalytically active hybrid nanostructures.

Conclusions

We have demonstrated that photochemical functionalization of vertically aligned carbon nanofibers with molecules that expose carboxylic acid groups greatly enhances the nucleation of electrocatalytically active Pt nanoparticles to the VACNF surfaces. The ability to enhance the nucleation of Pt nanoparticles without inhibiting the electrocatalytic activity is significant because it suggests that this approach may be applicable to a wide range of electrocatalytic problems. For example, while the molecular layer here was used to bind platinum nanoparticles to carbon nanofibers, this method could be utilized to bind catalytically active molecules to the surface of carbon nanofibers. The ability to use molecular monolayers to tune the chemical properties of the nanofibers without impeding the electron-transport properties opens a range of opportunities for formation of new types of catalytically active hybrid nanostructures.

Acknowledgment. This work is supported in part by the National Science Foundation grants DMR-0210806, DMR-0425880, and CHE-0613010. The authors thank Stacy E. Metz for assistance with the ICP-OES measurements.

References and Notes

(1) Kim, C.; Kim, Y. J.; Kim, Y. A.; Yanagisawa, T.; Park, K. C.; Endo, M.; Dresselhaus, M. S. *J. Appl. Phys.* **2004**, *96*, 5903.
(2) Arico, A. S.; Bruce, P.; Scrosati, B.; Tarascon, J. M.; Van Schalkwijk, W. *Nat. Mater.* **2005**, *4*, 366.
(3) Baughman, R.; Zakhidov, A.; de Heer, W. *Science* **2002**, *297*, 787.
(4) Harris, P. J. F. *Int. Mater. Rev.* **2004**, *49*, 31.
(5) Steigerwalt, E. S.; Deluga, G. A.; Lukehart, C. M. *J. Phys. Chem. B* **2002**, *106*, 760.
(6) Girishkumar, G.; Vinodgopal, K.; Kamat, P. V. *J. Phys. Chem. B* **2004**, *108*, 19960.
(7) He, Z. B.; Chen, J. H.; Liu, D. Y.; Tang, H.; Deng, W.; Kuang, W. F. *Mater. Chem. Phys.* **2004**, *85*, 396.
(8) Lian, S.; Holmes, K.-A.; Tsaprailis, H.; Birss, V. I. *J. Am. Chem. Soc.* **2006**, *128*, 3504.
(9) Tang, H.; Chen, J. H.; Yao, S. Z.; Nie, L. H.; Kuang, Y. F.; Huang, Z. P.; Wang, D. Z.; Ren, Z. F. *Mater. Chem. Phys.* **2005**, *92*, 548.
(10) Chen, Y.; Wang, Z. L.; Yin, J. S.; Johnson, D. J.; Prince, R. H. *Chem. Phys. Lett.* **1997**, *272*, 178.
(11) Endo, M.; Kim, Y. A.; Hayashi, T.; Fukai, Y.; Oshida, K.; Terrones, M.; Yanagisawa, T.; Higaki, S.; Dresselhaus, M. S. *Appl. Phys. Lett.* **2002**, *80*, 1267.
(12) Meyyappan, M.; Delzeit, L.; Cassell, A.; Hash, D. *Plasma Sources Sci. Technol.* **2003**, *12*, 205.
(13) Melechko, A. V.; Merkulov, V. I.; McKnight, T. E.; Guillorn, M. A.; Klein, K. L.; Lowndes, D. H.; Simpson, M. L. *J. Appl. Phys.* **2005**, *97*, 041301.
(14) McCreery, R. L. Carbon Electrodes: Strctural Effects on Electron Transfer Kinetics. In *Electroanalytical Chemistry;* Bard, A. J., Ed.; Marcel Dekker, Inc: 1990; Vol. 17, p 221.
(15) Banks, C. E.; Davies, T. J.; Wildgoose, G. G.; Compton, R. G. *Chem. Commun.* **2005**, 829.
(16) Tian, Z. Q.; Jiang, S. P.; Liang, Y. M.; Shen, P. K., *J. Phys. Chem. B* **2006**, *110*, 5343.
(17) Lakshminarayanan, P. V.; Toghiani, H.; Pittman, C. U. *Carbon* **2004**, *42*, 2433.

(18) Strother, T.; Knickerbocker, T.; Russell, J. N., Jr.; Butler, J. E.; Smith, L. M.; Hamers, R. J. *Langmuir* **2002**, *18*, 968.
(19) Baker, S. E.; Tse, K. Y.; Hindin, E.; Nichols, B. M.; Clare, T. L.; Hamers, R. J. *Chem. Mater.* **2005**, *17*, 4971.
(20) Baker, S. E.; Colavita, P. E.; Tse, K. Y.; Hamers, R. J. *Chem. Mater.* **2006**, *18*, 4415.
(21) Metz, K. M.; Tse, K. Y.; Baker, S. E.; Landis, E. C.; Hamers, R. J. *Chem. Mater.* **2006**, *18*, 5398.
(22) Baker, S. E.; Tse, K. Y.; Lee, C. S.; Hamers, R. J. *Diamond Relat. Mater.* **2006**, *15*, 433.
(23) Tse, K.-Y.; Baker, S. E.; Colavita, P. E.; Marcus, M. S.; Zhu, Y.; Voyles, P. M.; Hamers, R. J. *Langmuir* 2006, submitted for publication.
(24) Mallory, G. O.; Hajdu, J. B. *Electroless Plating: Fundamentals & Applications*; American Electroplaters and Surface Finishers Society: Orlando, FL, 1990.
(25) The tin bath contains 0.026 M $SnCl_2$ and 0.07 M trifluoroacetic acid in a 1:1 (by volume) mixture of methanol in deionized water.
(26) The Pt bath consists of 10 μL of diammineplatinum(II) nitrate (5 wt % solution, Strem) added to a 10 mL bath containing 1.92 M ammonium hydroxide, 0.4 M hydroxylamine hydrochloride, and 0.25 M hydrazine hydrate with pH = 11.95.
(27) Love, J. C.; Estroff, L. A.; Kriebel, J. K.; Nuzzo, R. G.; Whitesides, G. M. *Chem. Rev.* **2005**, *105*, 1103.
(28) Boubour, E.; Lennox, R. B. *Langmuir* **2000**, *16*, 4222.
(29) Barrelet, C. J.; Robinson, D. B.; Cheng, J.; Hunt, T. P.; Quate, C. F.; Chidsey, C. E. D. *Langmuir* **2001**, *17*, 3460.
(30) Cheng, J.; Robinson, D. B.; Cicero, R. L.; Eberspacher, T.; Barrelet, C. J.; Chidsey, C. E. D. *J. Phys. Chem. B* **2001**, *105*, 10900.
(31) Yu, H. Z.; Morin, S.; Wayner, D. D. M.; Allongue, P.; de Villeneuve, C. H. *J. Phys. Chem. B* **2000**, *104*, 11157.
(32) Tse, K. Y.; Nichols, B. M.; Yang, W. S.; Butler, J. E.; Russell, J. N., Jr.; Hamers, R. J. *J. Phys. Chem. B* **2005**, *109*, 8523.
(33) Cline, K. K.; McDermott, M. T.; McCreery, R. L. *J. Phys. Chem.* **1994**, *98*, 5314.
(34) Kneten, K. R.; McCreery, R. L. *Anal. Chem.* **1992**, *64*, 2519.
(35) Kuo, T. C.; McCreery, R. L. *Anal. Chem.* **1999**, *71*, 1553.
(36) Ranganathan, S.; McCreery, R. L. *Anal. Chem.* **2001**, *73*, 893.
(37) Bergamaski, K.; Pinheiro, A. L. N.; Teixeira-Neto, E.; Nart, F. C. *J. Phys. Chem. B* **2006**, *110*, 19271.
(38) Kuk, S. T.; Wieckowski, A. *J. Power Sources* **2005**, *141*, 1.
(39) Park, S.; Wasileski, S. A.; Weaver, M. J. *Electrochim. Acta* **2002**, *47*, 3611.
(40) Yahikozawa, K.; Fujii, Y.; Matsuda, Y.; Nishimura, K.; Takasu, Y. *Electrochim. Acta* **1991**, *36*, 973.
(41) Ota, K. I.; Nakagawa, Y.; Takahashi, M. *J. Electroanal. Chem.* **1984**, *179*, 179.
(42) Lu, G. Q.; Chrzanowski, W.; Wieckowski, A. *J. Phys. Chem. B* **2000**, *104*, 5566.
(43) Lopes, M. I. S.; Beden, B.; Hahn, F.; Leger, J. M.; Lamy, C. *J. Electroanal. Chem.* **1991**, *313*, 323.
(44) Herrero, E.; Franaszczuk, K.; Wieckowski, A. *J. Phys. Chem.* **1994**, *98*, 5074.
(45) Song, S.; Wang, G.; Zhou, W.; Zhao, X.; Sun, G.; Xin, Q.; Kontou, S.; Tsiakaras, P. *J. Power Sources* **2005**, *140*, 103.
(46) Stevens, F.; Kolodny, L. A.; Beebe, T. P. *J. Phys. Chem. B* **1998**, *102*, 10799.